

## Original Paper

# Involvement of Endoplasmic Reticulum Stress in Uremic Cardiomyopathy: Protective Effects of Tauroursodeoxycholic Acid

Wei Ding<sup>a</sup> Bin Wang<sup>b</sup> Minmin Zhang<sup>b</sup> Yong Gu<sup>b</sup><sup>a</sup>Division of Nephrology, Shanghai Ninth People's Hospital, School of Medicine, Shanghai Jiaotong University, Shanghai, <sup>b</sup>Division of Nephrology, Huashan Hospital and Institute of Nephrology, Fudan University, Shanghai, China**Key Words**

Chronic kidney disease • Uremic cardiomyopathy • Endoplasmic reticulum stress • Apoptosis • TUDCA

**Abstract**

**Background/Aims:** Uremic cardiomyopathy (UCM) is a complication in chronic kidney disease. We investigated if endoplasmic reticulum stress (ERS) is involved in UCM, and determined the efficacy of tauroursodeoxycholic acid (TUDCA) in UCM prevention. **Methods:** Mice were divided randomly into three groups: sham (saline, i.p.), 5/6 nephrectomized (Nx) (saline, i.p.) and Nx+TUDCA (250 mg/kg/day, i.p.). Renal function was assessed by measuring serum creatinine, blood urea nitrogen and by periodic acid-Schiff reagent staining. Histologic examination of cardiac fibrosis and apoptosis was determined by Masson's trichrome and TUNEL assay. Cardiac function was evaluated by echocardiography. Fibrotic factors (transforming growth factor- $\beta$ , fibronectin, collagen I/IV) were evaluated by real-time PCR. ERS-related proteins were measured by western blotting. **Results:** Impaired renal function and cardiac dysfunction were shown in 5/6 nephrectomy mice but were improved significantly by TUDCA. 5/6 nephrectomy mice exhibited marked cardiomyocyte apoptosis, cardiac fibrosis and elevated pro-fibrotic factors. ERS markers (GRP78, GRP94, P-PERK, P-eIF2a) and ERS-induced apoptosis pathways (activation of CHOP and caspase-12) were increased significantly in 5/6 nephrectomy mice, and TUDCA treatment blunted these changes. **Conclusions:** ERS has a key role in UCM, and the cardioprotective role of TUDCA is related to inhibition of ERS-induced apoptosis by inhibition of CHOP and caspase-12 pathways.

© 2016 The Author(s)  
Published by S. Karger AG, Basel**Introduction**

Chronic kidney disease (CKD) carries a high burden of morbidity and mortality. Cardiovascular complications are important clinical problems in CKD patients. Recent

Minmin Zhang

Division of Nephrology, Huashan Hospital and Institute of Nephrology, Fudan University, 12 Wulumuqi Road, Shanghai 200040, (China)  
Tel. +862152888133, Fax +86 2162268509, E-Mail zhangminmin03@126.com

reports have demonstrated that > 40% of deaths among patients with end-stage renal disease is due to cardiovascular disease (CVD) [1]. Gansevoort et al. stated that the renin-angiotensin-aldosterone system, uremic toxins, inflammation, oxidative stress, and anemia play key parts in the pathogenesis of cardiac disease in CKD [2]. The uremic *milieu* carries several risk factors for cardiac disease that can give rise to uremic cardiomyopathy (UCM) [3]. Cross-sectional studies have demonstrated that left-ventricular hypertrophy (LVH), an independent risk factor for survival, is the most prevalent cardiac alteration in CKD [4]. LVH is a well-recognized risk factor for CVD, but CKD patients develop LVH early in the progression of renal disease [5]. In CKD patients, cardiac remodeling is characterized by alteration in the shape, size and function of the heart in response to cardiac injury. Cardiomyocytes and fibroblasts are also involved in the development of cardiac remodeling, and increased apoptosis of cardiomyocytes and upregulated synthesis of collagen eventually leads to cardiac fibrosis [6]. However, the exact mechanisms of UCM are incompletely understood.

Cardiomyocyte apoptosis plays an important part in cardiac remodeling and leads to systolic dysfunction or even sudden death [7]. The endoplasmic reticulum (ER) mediates apoptosis in response to various types of stress [8]. The ER participates in protein folding, Ca<sup>2+</sup> homeostasis, biosynthesis of lipids, and the stress response in many mammalian cell types. Excessive misfolding or unfolding of proteins in the ER result in activation of transmembrane sensors (e.g., inositol-requiring enzyme-1 $\alpha$  (IRE-1 $\alpha$ ), RNA-dependent protein kinase-like ER kinase (PERK) and activating transcription factor (ATF6)), which in turn activate endoplasmic reticulum stress (ERS) [9]. However, prolonged or excessive ERS initiates apoptosis pathways, such as transcriptional induction of CCAAT/enhancer-binding protein (C/EBP) homologous protein (CHOP/GADD153), as well as activation of c-Jun NH<sub>2</sub>-terminal kinase and a caspase-12-dependent pathway [10]. Recently, ERS-induced apoptosis has been implicated as a major factor in various types of cardiovascular disorders: cardiac hypertrophy, cardiac failure, ischemic heart disease, and atherosclerosis [11–15].

Tauroursodeoxycholic acid (TUDCA) is an endogenous bile acid and considered to be a potential inhibitor of apoptotic signaling. A growing body of evidence has demonstrated that TUDCA, as a “molecular chaperone”, can prevent prolonged ERS directly by inhibiting the unfolded protein response (UPR) and its downstream pathway [16, 17]. However, the protective role of TUDCA in UCM is not clear.

Here, we wished to: (i) ascertain if ERS-induced cardiomyocyte apoptosis and its downstream signaling pathway are involved in UCM; (ii) investigate the potential role of TUDCA treatment in uremic-induced cardiomyocyte injury.

## Materials and Methods

The study protocol was approved by the Ethics Committee of Fudan University (Shanghai, China). Experiments were conducted according to Guidelines for the Care and use of Animals (National Institutes of Health, Bethesda, MD, USA).

### *Animal model and experimental protocol*

According to Cheung's study, kidney ablation (5/6 nephrectomy (Nx)) was carried out in male C57BL/6J mice (22–25 g) [18]. All mice were divided randomly into three groups: (i) sham-operated and injected with physiologic (0.9%) saline as vehicle (Sham+V); (ii) 5/6 nephrectomy-operated and injected with 0.9% saline as vehicle (Nx+V); (iii) Nx mice treated with TUDCA (250 mg/kg/day, i.p.) (Nx+TUDCA) [17]. Administration of 0.9% saline or TUDCA was continued to 12 weeks. Serum creatinine (sCr) was measured using enzyme-linked immunoassay kits (Exocell, Philadelphia, PA, USA) according manufacturer instructions, and blood urea nitrogen (BUN) was measured using urease methods (BioTNT company, Shanghai, China).

#### Histologic examination

Samples of kidney tissue (thickness, 4  $\mu$ m) were fixed in 4% paraformaldehyde and embedded in paraffin. Then, they were stained with periodic acid-Schiff reagent (PAS) according to standard procedures. Specific criteria were used for tissue grading: 0, no abnormality; 1+, minor (segmental lesion < 25%); 2+, mild (25 – 50%); 3+, moderate (51 – 75%); 4+, severe (> 75%, diffuse proliferation and nearly complete sclerosis). A minimum of 20 glomeruli was assessed in each specimen [19]. Fresh samples of left ventricles were also fixed using 4% paraformaldehyde and embedded in paraffin, and then cut into slices of thickness 4  $\mu$ m. Total collagen content in myocardial tissue was determined by staining with Masson's trichrome. Results are shown as the percentage of total myocardial area, and the ratio of collagen fiber: muscular tissue was calculated [20, 21]. All histologic examinations were undertaken in a blinded fashion.

#### Echocardiographic evaluation

Echocardiography was carried out to detect the development of UCM after 12 weeks. M-mode echocardiography was undertaken using a high-resolution imaging system (Vevo 770<sup>®</sup>; Fujifilm VisualSonics, Tokyo, Japan) and a 30-MHz mechanical transducer. Mice were anesthetized and maintained at a body temperature of 37°C during the non-invasive imaging procedure. The echocardiographic parameters measured were: heart rate (HR); left-ventricular ejection fraction (LVEF); left-ventricular fractional shortening (LVFS); left-ventricular internal dimension systole (LVIDs); left-ventricular internal dimension diastole (LVIDd); left-ventricular diastolic posterior wall thickness (LVPWd); left-ventricular systolic posterior wall thickness (LVPWs).

#### Real-time polymerase chain reaction (PCR)

Total RNA was extracted from the heart using an RNA Isolation kit (Invitrogen, Carlsbad, CA, USA) according to manufacturer instructions. Reverse transcription of RNA was done using a First-stand cDNA Synthesis kit (Fermentas, Waltham, MA, USA). Gene expression was measured using a 7500 Detection System (Applied Biosystems, Foster City, CA, USA). Oligonucleotides were designed and synthesized by Invitrogen (Table 1). The comparative  $2^{-\Delta\Delta CT}$  method was used to calculate the relative amounts of target genes.

#### Terminal deoxynucleotidyl transferase-mediated dUTP nick-end labeling (TUNEL) assay

Cardiomyocyte apoptosis was detected using a TUNEL kit (Roche, Basel, Switzerland) according to manufacturer instructions. In brief, after deparaffinization and rehydration, sample sections were treated with protease K (20  $\mu$ g/mL) for 15 min. Then, slides were immersed in a TUNEL reaction mixture for 60 min in the dark at 37°C. Slides were assessed by fluorescence microscopy. The TUNEL Index was calculated as the ratio of the number of TUNEL-positive cells divided by the total number of cells. At least ten random fields were evaluated in each location of the heart (magnification,  $\times$  400).

#### Western blotting

Western blotting of heart tissue was undertaken as described previously [22]. After blotting, membranes were incubated overnight with antibodies against GRP78 (1:1000 dilution; Cell Signaling Technology, Beverly, MA, USA); GRP94 (1:1000; Cell Signaling Technology); P-PERK (1:1000; Cell Signaling

**Table 1.** Oligonucleotides synthesized by Invitrogen (Carlsbad, CA, USA)

	Forward	Reverse
Transforming growth factor-beta	5'-AGCTTTGCAGGGTGGGTATC-3'	5'-CCTTCGGGTGAGACCACAAA-3'
Fibronectin	5'-GCGACGGTATTCTGTAAAGTGG-3'	5'-GGACAGGGCTTTGGCAGTT-3'
Collagen I	5'-AGGGTCATCGTGGCTTCTCT-3'	5'-CAGGCTCTTGAGGGTAGTGT-3'
Collagen IV	5'-ATCGGATACTCCTTCCTCATGC-3'	5'-CCAGGGGAGACTAGGGACTG-3'
Glyceraldehyde 3-phosphate dehydrogenase	5'-TCAGCCGCATCTTCTTTTG-3'	5'-AAATCCGTTGACTCCGACC-3'

Technology); P-eIF2a (1:1000; Cell Signaling Technology); CHOP (1:500; Santa Cruz Biotechnology, Santa Cruz, CA, USA) and caspase-12 (1:500; Santa Cruz Biotechnology). After washing, blots were incubated with secondary antibody for 2 h. Membranes were visualized with an enhanced chemiluminescent system (Amersham, Little Chalfont, UK) and band intensity quantified using Quantity One (Bio-Rad, Hercules, CA, USA).

#### Statistical analyses

Data were expressed as means  $\pm$  the standard error of the mean (SEM). One-way ANOVA was used to compare mean values, and significance was accepted when  $p < 0.05$ .

## Results

### Impaired renal function in Nx mice is improved in Nx+TUDCA mice

Renal damage was evaluated by PAS staining, sCr level, and BUN level. Compared with the Sham+V group (Glomerular Injury Score,  $0.19 \pm 0.06$ ), Nx+V mice exhibited significantly expanded mesangial regions and glomerulosclerosis ( $3.41 \pm 0.12$ ) (Fig. 1). However, treatment with TUDCA markedly improved kidney damage and decreased the Glomerular Injury Score ( $0.87 \pm 0.07$ ) (Fig. 1A–D). Similarly, levels of sCr and BUN were increased in Nx+V mice ( $0.86 \pm 0.05$  and  $81.63 \pm 3.18$  mg/dL, respectively) compared with Sham+V mice ( $0.15 \pm 0.01$  and  $22.16 \pm 0.93$  mg/dL, respectively). Levels of sCr and BUN were reduced in Nx+TUDCA mice ( $0.49 \pm 0.03$  and  $44.58 \pm 2.07$  mg/dL, respectively) compared with Nx+V mice (Fig. 1E, F).

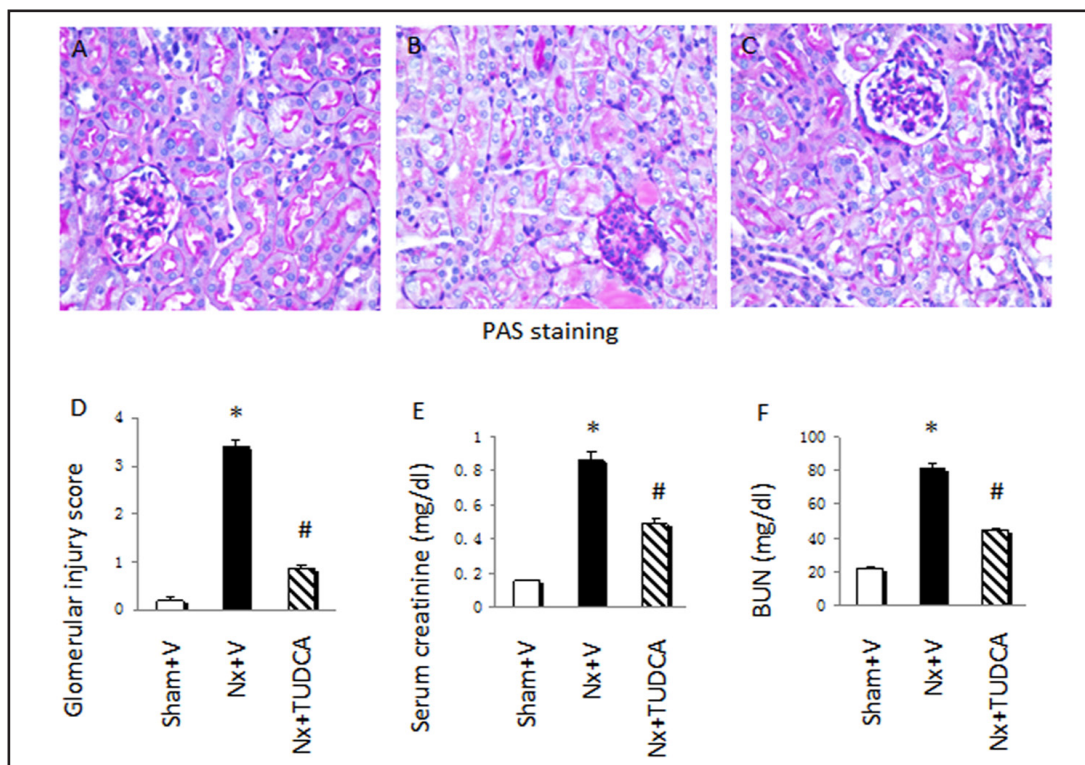


**Fig. 1.** Physiologic parameters in mice at the end of the 12-week study. Representative photomicrographs (magnification  $\times 400$ ) of PAS-stained kidney sections (A–D). (A) Sham+V group; (B) Nx+V group; (C) Nx+TUDCA group; (D) Glomerular Injury Score; (E) serum creatinine; (F) BUN. Data are the mean  $\pm$  SEM ( $n = 6$ ). \*  $P < 0.05$ , Sham+V vs. Nx+V group; #  $P < 0.05$ , Nx+V group vs. Nx+TUDCA group.

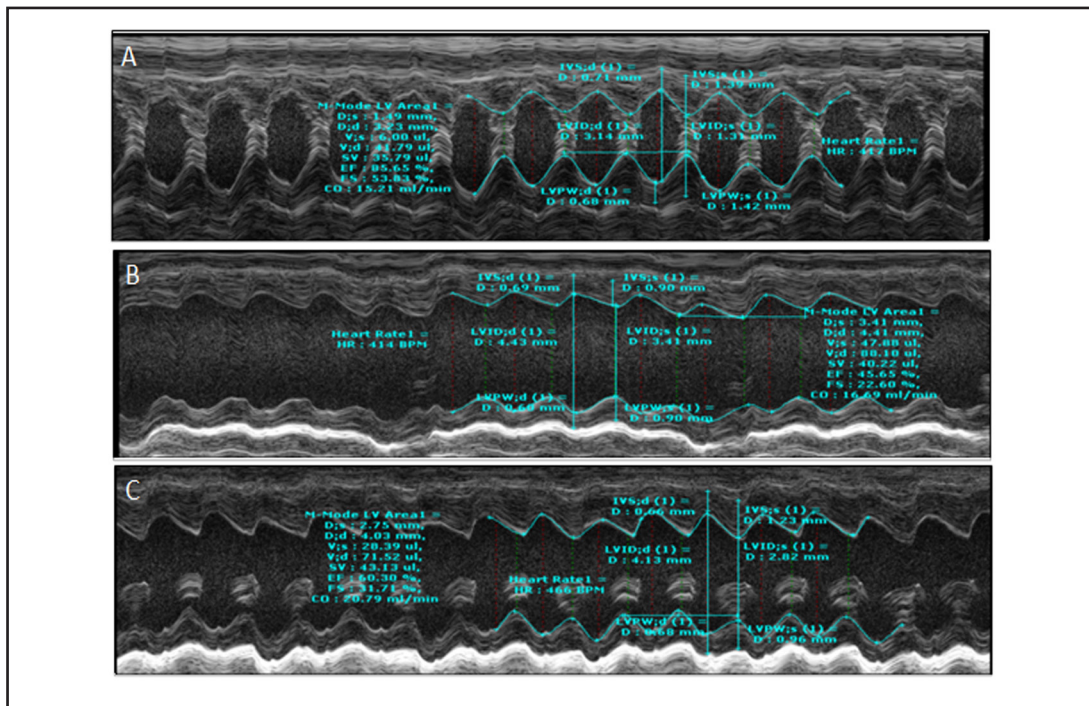


**Fig. 2.** General characteristics and echocardiography features across all groups. (A) Sham+V group; (B) Nx+V group; (C) Nx+TUDCA group.

**Table 2.** Echocardiographic parameters at week-12. HR: heart rate; LVEF: left-ventricular ejection fraction; LVFS: left-ventricular fractional shortening; LVIDs: left-ventricular internal dimension systole; LVIDd: left-ventricular internal dimension diastole; LVPWd: left-ventricular diastolic posterior wall thickness; LVPWs: left-ventricular systolic posterior wall thickness. Data are the mean  $\pm$  SEM; (n = 6); \* P < 0.05, Sham+V vs. Nx+V; # P < 0.05, Nx+V vs. Nx+TUDCA

Parameter	Sham+V	Nx+V	Nx+TUDCA
HR (bpm)	448.00 $\pm$ 16.09	464.67 $\pm$ 25.35	459.33 $\pm$ 15.19
LVEF (%)	82.23 $\pm$ 1.75	41.52 $\pm$ 2.11*	57.98 $\pm$ 1.48#
LVFS (%)	50.28 $\pm$ 1.83	23.06 $\pm$ 2.53*	34.33 $\pm$ 3.27#
LVIDs (mm)	1.67 $\pm$ 0.21	3.92 $\pm$ 0.32*	2.53 $\pm$ 0.25#
LVIDd (mm)	3.26 $\pm$ 0.20	5.30 $\pm$ 0.45*	3.91 $\pm$ 0.17#
LVPWd (mm)	0.72 $\pm$ 0.032	0.75 $\pm$ 0.084	0.67 $\pm$ 0.026
LVPWs (mm)	1.30 $\pm$ 0.12	1.85 $\pm$ 0.47	1.55 $\pm$ 0.29

### General characteristics and echocardiography

Cardiac changes as detected by echocardiography are shown in Fig. 2 and Table 2. LVEF and LVFS in Nx+V mice were reduced significantly compared with Sham+V mice at week-12. TUDCA treatment improved the values of LVEF and LVFS significantly. LVIDs and LVIDd were increased significantly in Nx+V mice compared with Sham+V mice. However, TUDCA treatment decreased these parameters markedly. HR, LVPWd and LVPWs in Sham+V mice and Nx+V mice were not significantly different throughout the experiment.

**Fig. 3.** Collagen content in left-ventricular tissues of mice. Representative photomicrographs of Masson's trichrome-stained heart sections (A–C). (A) Sham+V group; (B) Nx+V group; (C) Nx+TUDCA group; (D) area of cardiac fibrosis (%) was evaluated as described in the Material and Methods section. Values are the mean  $\pm$  SEM (n = 6). \* P < 0.05, Sham+V vs. Nx+V group; # P < 0.05, Nx+V group vs. Nx+TUDCA group. Magnification  $\times$  400.

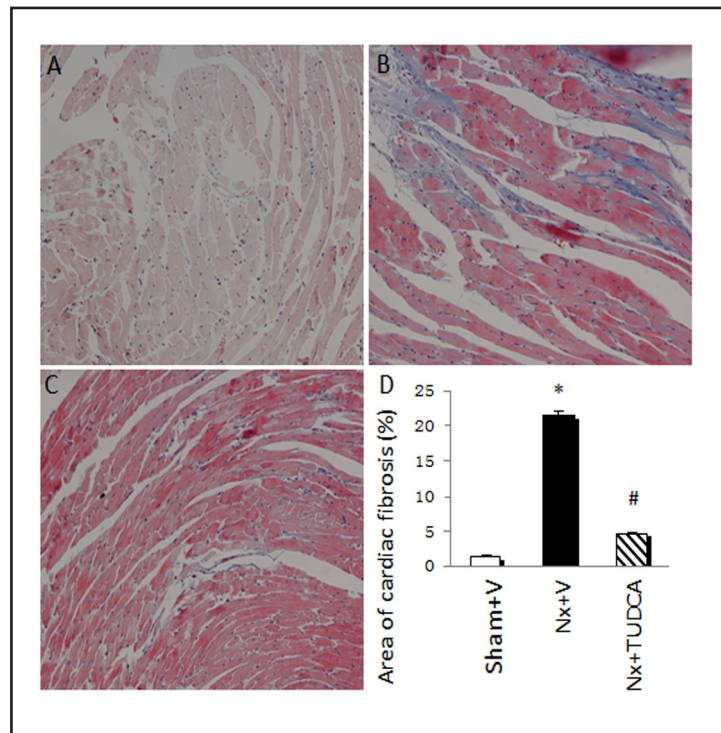
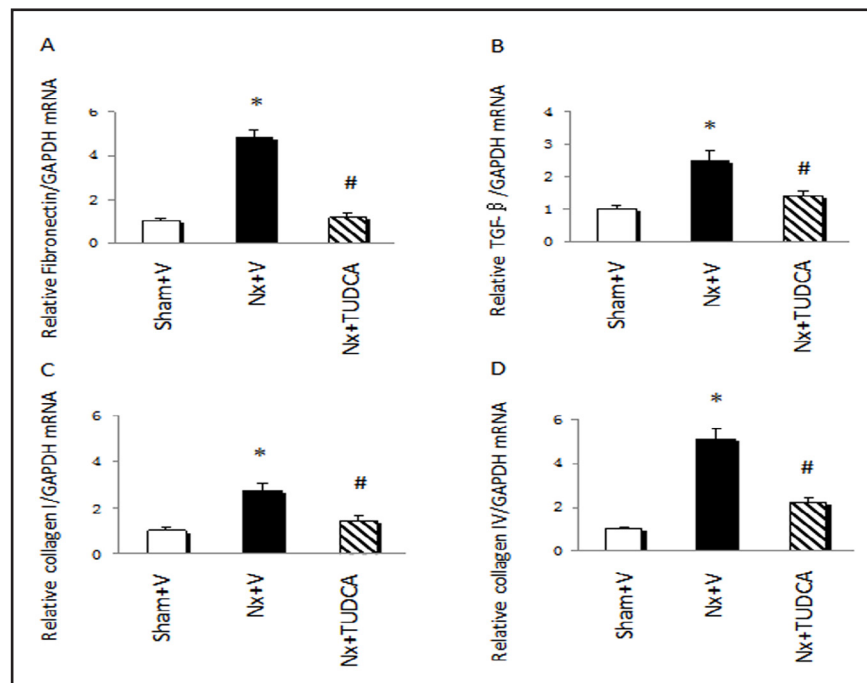


**Fig. 4.** Expression of inflammatory cytokines in the heart. mRNA expression of fibronectin (A), TGF- $\beta$  (B), collagen I (C) and collagen IV (D) was detected by real-time PCR and normalized to expression of glyceraldehyde 3-phosphate dehydrogenase. Values are the mean  $\pm$  SEM (n = 6). \* P < 0.05, Sham+V vs. Nx+V group; # P < 0.05, Nx+V group vs. Nx+TUDCA group.



#### Effects of TUDCA on cardiac fibrosis

Compared with the Sham+V group, Nx+V mice showed a significant increase in interstitial myocardial collagen content upon staining by Masson's trichrome (Fig. 3). However, TUDCA-treated mice exhibited lower interstitial myocardial collagen content. Similar results between these two groups of mice were observed using real-time PCR. mRNA levels of fibronectin, transforming growth factor (TGF)- $\beta$ , collagen I, and collagen IV were elevated significantly in Nx+V mice (4.8-, 2.5-, 2.7- and 5.1-fold, respectively) than in Sham+V

**Fig. 5.** TUNEL assay in all groups. (A) Sham+V group; (B) Nx+V group; (C) Nx+TUDCA group; (D) quantitative analysis of myocardial apoptosis in all groups. Apoptotic nuclei are stained red, and the TUNEL Index was calculated as the ratio of TUNEL-positive cells divided by the total number of cells. Values are the mean  $\pm$  SEM (n = 6). \* P < 0.05, Sham+V vs. Nx+V group; # P < 0.05, Nx+V group vs. Nx+TUDCA group. Magnification  $\times$  400.

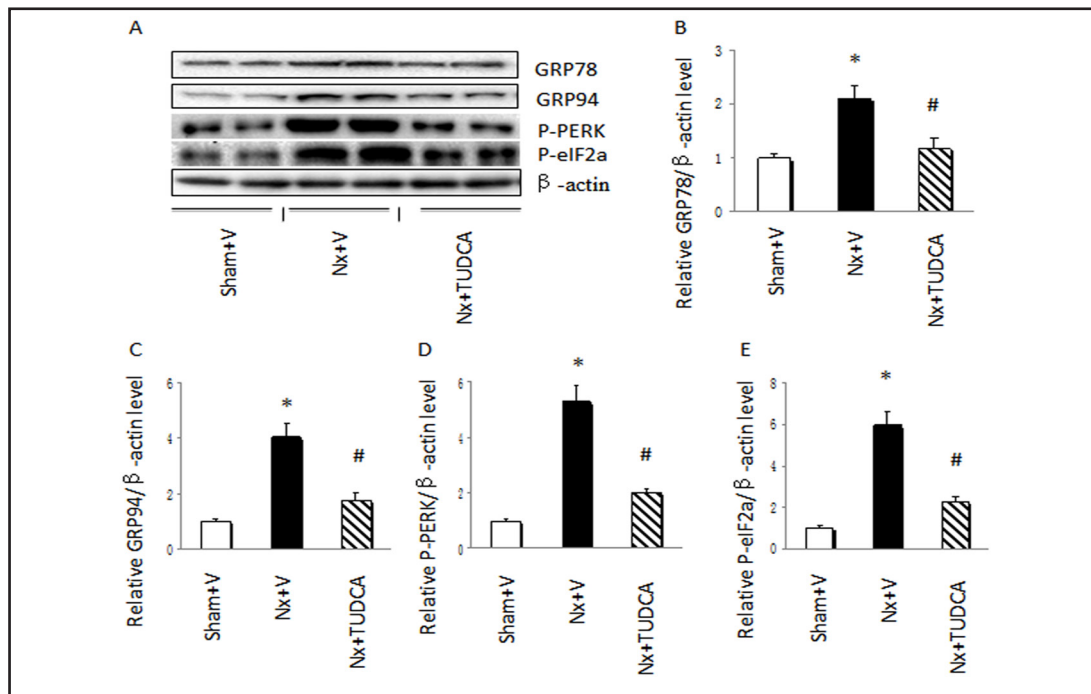
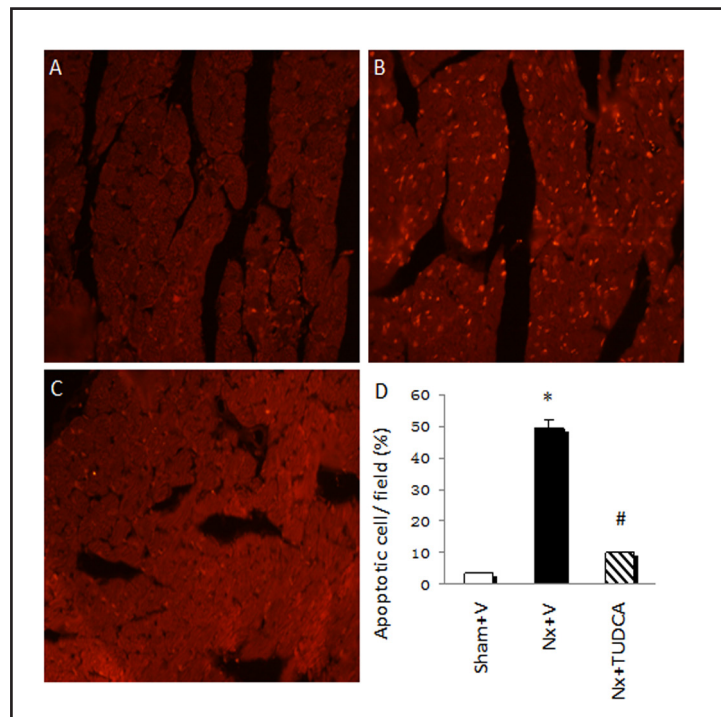


**Fig. 6.** TUDCA ameliorated uremia-induced ERS in cardiomyocytes. (A) Representative western blots of GRP78, GRP94, P-PERK and P-eIF2a. (B) Relative expression of GRP78 to expression of  $\beta$ -actin. (C) Relative expression of GRP94 to expression of  $\beta$ -actin. (D) Relative expression of P-PERK to expression of  $\beta$ -actin. (E) Relative expression of P-eIF2a to expression of  $\beta$ -actin. Values are the mean  $\pm$  SEM (n = 6). \* P < 0.05, Sham+V vs. Nx+V group; # P < 0.05, Nx+V group vs. Nx+TUDCA group.

mice, and TUDCA treatment markedly reduced mRNA levels of fibronectin, TGF- $\beta$ , collagen I and collagen IV relative to those of Nx+V mice (Fig. 4).

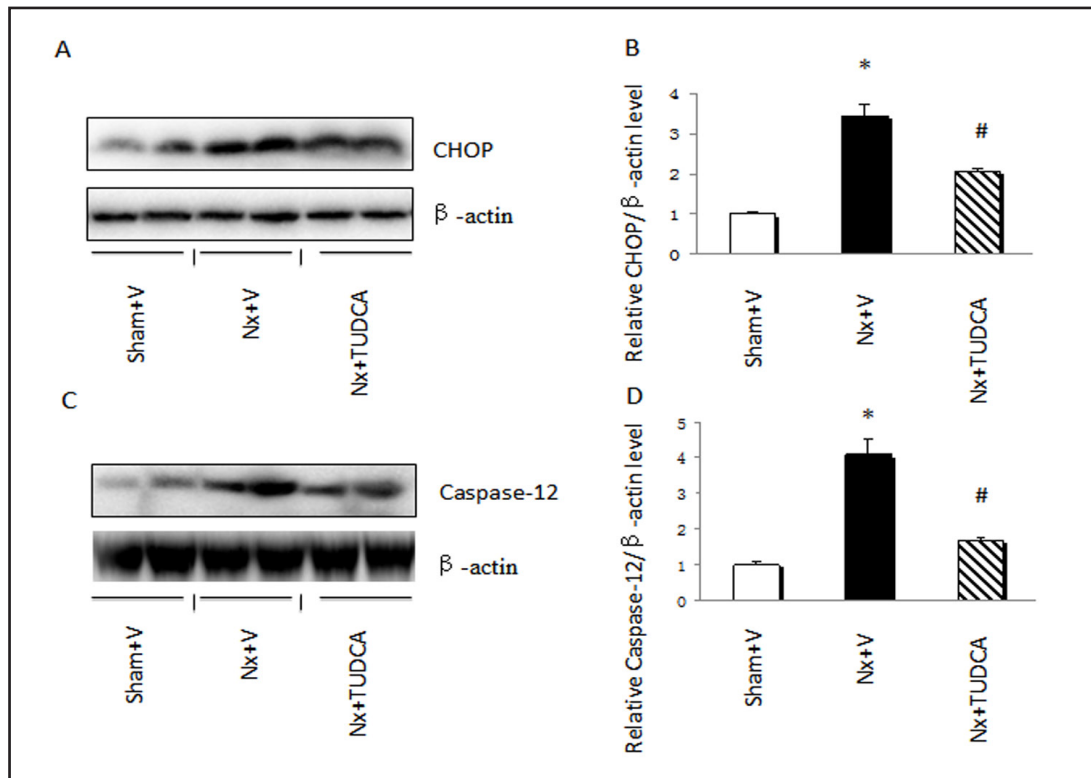


**Fig. 7.** TUDCA inhibited an ERS-induced apoptotic pathway in cardiomyocytes. (A) Representative western blots of CHOP. (B) Relative expression of CHOP to β-actin expression. (C) Representative western blots of caspase-12. (D) Relative expression of caspase-12 to β-actin expression. Values are the mean ± SEM (n = 6). \* P < 0.05, Sham+V vs. Nx+V group; # P < 0.05, Nx+V group vs. Nx+TUDCA group.

#### *TUDCA reduced uremia-induced apoptosis in mouse heart*

Apoptosis has a key role in myocardial remodeling and leads to cardiac dysfunction. Hence, we observed the effects of TUDCA on apoptosis in mouse hearts. The ratio of TUNEL-positive cardiomyocytes in Nx+V mice ( $49.1 \pm 2.66$ ) was significantly higher than that in the Sham+V group ( $3.6 \pm 0.22$ ) (Fig. 5). TUDCA administration reduced the percentage of TUNEL-positive cells at week-12 significantly, suggesting that chronic treatment with TUDCA can ameliorate uremia-induced apoptosis of cardiomyocytes.

#### *Effects of TUDCA on ERS markers in mouse cardiomyocytes*

The proteins GRP78 and GRP 94 are central regulators of ER function and used widely as ERS markers. Compared with the Sham+V group, expression of GRP78 (2.1-fold) and GRP94 (4.0-fold) increased significantly in mouse hearts from the Nx+V group, whereas TUDCA treatment decreased levels of GRP78 and GRP94 markedly (Fig. 6A–C). Increased activation of P-PERK (5.3-fold) and P-eIF2a (5.9-fold) in mouse hearts from the Nx+V group was observed compared with the Sham+V group. However, TUDCA treatment decreased levels of P-PERK and P-eIF2a significantly (Fig. 6C–D).

#### *Effects of TUDCA on ERS-induced apoptotic pathway in mouse cardiomyocytes*

High levels of ERS can induce apoptosis through CHOP and caspase-12 pathways. We measured levels of CHOP and caspase-12 in mouse hearts. Compared with the Sham+V group, levels of CHOP (3.4-fold) and caspase-12 (4.1-fold) were increased significantly in the Nx+V group, whereas TUDCA treatment decreased levels of CHOP and caspase-12 markedly (Fig. 7), suggesting the important role of CHOP and caspase-12 signaling in UCM progression.

## Discussion

Chronic heart failure is considered to be the major cause of cardiovascular death in patients with CKD and end-stage renal disease [23]. UCM is characterized by cardiomyocyte apoptosis and interstitial myocardial fibrosis [24]. However, the various pathways responsible for cardiomyocyte apoptosis in etiologically different cardiac diseases (including UCM) have not been identified.

In the present study, significant renal dysfunction, left-ventricular dysfunction, and UCM were demonstrated in mice after 5/6 nephrectomy. We also demonstrated that UCM is mediated by ERS and ERS-induced apoptosis in an *in vivo* study. According to Gupta S's research, TUDCA could prevent acute kidney injury in rat and cell culture models through anti-apoptotic properties [25]. In present study, we found that TUDCA treatment ameliorated renal injury, heart dysfunction and interstitial myocardial fibrosis significantly, and attenuated ERS and ERS-induced cardiomyocyte apoptosis markedly by inhibiting CHOP and caspase-12 signaling pathways. Our research suggests that TUDCA could be a new therapeutic agent for UCM or other cardiac diseases.

5/6 nephrectomy is a classic model of end-stage renal disease. In the present study, sCr level, BUN level and scores for PAS staining were increased significantly in 5/6 nephrectomy mice. 5/6 nephrectomy also induced dysfunction and remodeling of the left ventricle, which was accompanied by cardiomyocyte apoptosis and myocardial interstitial fibrosis.

The pathogenesis of UCM is incompletely understood. TGF- $\beta$  is a key mediator in fibrosis of solid organs, and has been implicated in UCM progression [26]. In our 5/6 nephrectomy model, renal dysfunction led to cardiomyocyte apoptosis and myocardial fibrosis as detected by the TUNEL assay and staining with Masson's trichrome. Levels of several factors denoting fibrosis in heart tissue, including TGF- $\beta$ , fibronectin, collagen I and collagen IV, were increased significantly in the 5/6 nephrectomy group. TUDCA treatment could not only attenuate left-ventricular dysfunction and renal injury, but also decreased cardiomyocyte apoptosis and myocardial fibrosis.

The transmembrane proteins IRE-1a, PERK, ATF6 are components of ERS and play vital parts in the maintenance of ER function. In health, IRE-1a, PERK and ATF6 combine with GRP78 or other chaperone molecular proteins. GRP78 is considered to be a key chaperone protein during ERS, and has been widely used as an ERS marker [27]. When cells were under ERS, GRP78 then binding increased misfolded or unfolded protein and released from the ERS sensor protein, eventually led to IRE-1a, PERK and ATF6 activation [28]. Activation of ATF-6 and IRE-1 can increase transcription of UPR-related genes; PERK prevents ERS mainly by initiating the phosphorylation of eIF2 $\alpha$  protein directly [29, 30]. If eIF2 is phosphorylated by PERK, it then binds to eIF2B and prevents recycling of eIF2-GDP to eIF2-GTP. The lower level of eIF-GTP inhibits assembly of the 43S translation initiation complex and prevents synthesis of misfolded or unfolded proteins [31, 32]. In the present study, expression of the chaperone proteins GRP78 and GRP94 was increased markedly in our animal model of UCM, and activation of P-PERK and P-eIF2 $\alpha$  was also increased significantly. However, TUDCA treatment could decrease expression of these ERS markers and transmembrane proteins significantly. These data suggest that the PERK/eIF2 $\alpha$  pathway has an important role in UCM.

Apoptosis is also involved in myocardial stress (including ventricular remodeling). Inhibition of cardiomyocyte apoptosis is considered to be a key treatment target of myocardial injury [33]. Various signaling pathways have been implicated in cardiomyocyte apoptosis. Of these apoptosis pathways, CHOP is one of the most important, and is related to ERS. CHOP protein belongs to the C/EBP family of transcription factors. Activated ATF-6 can induce activation of CHOP, which is also a downstream target of X-box binding protein (XBP)-1 [34]. A growing body of evidence suggests that CHOP overexpression can promote apoptosis, and that CHOP deficiency can protect cells against ERS-induced apoptosis [35, 36]. Previously, we showed that CHOP-mediated ERS contributes to aldosterone-induced apoptosis in tubular epithelial cells [37]. Taken together, CHOP appears to have a key role in the apoptosis caused by ERS. Furthermore, Okada et al. demonstrated that a CHOP-mediated

ERS apoptotic pathway is involved in murine heart failure [38]. CHOP signaling has also been shown to be involved in myocardial apoptosis in streptozocin-induced diabetic rats [39]. In the present study, we focused on CHOP-mediated apoptotic signaling in UCM. We observed that activation of CHOP and apoptosis was increased significantly in the 5/6 nephrectomy group compared with mice in the Sham group. TUDCA treatment could inhibit CHOP activation and decrease cardiomyocyte apoptosis as confirmed by a reduction in the number of TUNEL-positive cardiomyocytes. Caspase-12 is localized exclusively in the ER and plays a key part in ERS-induced apoptosis. Activated caspase-12 can cleave procaspase-9 into active caspase-9, which in turn activates procaspase-3, eventually leading to apoptosis [40]. Caspase-12-mediated apoptosis is a specific pathway of ERS because membrane- or mitochondrial-targeted signaling cannot activate caspase-12 [41]. m-calpain may be involved in precursor cleavage of caspase-12. If cells undergo ERS,  $Ca^{2+}$  is transferred into the ER membrane and m-calpain is activated. This process initiates activation of the caspase-12 precursor and, eventually, cleaved caspase-12 starts activation of a caspase-3 cascade [42]. Our results demonstrated that expression of cleaved caspase-12 and cardiomyocyte apoptosis were increased significantly in the 5/6 nephrectomy group compared with sham group, and that TUDCA treatment could attenuate ERS and UCM.

## Conclusion

The present study showed that ERS-associated signaling was involved in UCM, probably by increasing expression of ERS-related transmembrane proteins (P-PERK, P-eIF2a) and by activating CHOP and caspase-12 pathways, thereby leading to cardiomyocyte apoptosis in UCM. Treatment with TUDCA could reduce cardiomyocyte apoptosis in the hearts of 5/6 nephrectomized mice. These data may provide important new insights into the cardioprotective role of TUDCA, and could lead to development of a therapeutic agent for UCM or other cardiac diseases.

## Acknowledgments

This work was supported by a grant from the National Natural Science Foundation of China (81270822, 81270009 and 81300590).

## Disclosure Statement

The authors declare that there is no conflict of interest.

## References

- 1 Foley RN, Parfrey PS, Sarnak MJ: Clinical epidemiology of cardiovascular disease in chronic renal disease. *Am J Kidney Dis* 1998;32:s112-119.
- 2 Gansevoort RT, Correa-Rotter R, Hemmelgarn BR, Jafar TH, Heerspink HJ, Mann JF, Matsushita K, Wen CP: Chronic kidney disease and cardiovascular risk: epidemiology, mechanisms, and prevention. *Lancet* 2013;382:339-352.
- 3 Semple D, Smith K, Bhandari S, Seymour AM: Uremic cardiomyopathy and insulin resistance: a critical role for akt? *J Am Soc Nephrol* 2011;22:207-215.
- 4 Silberberg JS, Barre PE, Prichard SS, Sniderman AD: Impact of left ventricular hypertrophy on survival in end-stage renal disease. *Kidney Int* 1989;36:286-290.
- 5 McMahan LP, Roger SD, Levin A; Slimheart Investigators Group: Development, prevention, and potential reversal of left ventricular hypertrophy in chronic kidney disease. *J Am Soc Nephrol* 2004;15:1640-1647.

- 6 Cohn JN, Ferrari R, Sharpe N: Cardiac remodeling-concepts and clinical implications: a consensus paper from an international forum on cardiac remodeling. Behalf of an international forum on cardiac remodeling. *J Am Coll Cardiol* 2000;35:569-582.
- 7 Wencker D, Chandra M, Nguyen K, Miao W, Garantziotis S, Factor SM, Shirani J, Armstrong RC, Kitsis RN: A mechanistic role for cardiac myocyte apoptosis in heart failure. *J Clin Invest* 2003;111:1497-1504.
- 8 Ron D: Translational control in the endoplasmic reticulum stress response. *J Clin Invest* 2002;110:1383-1388.
- 9 Xu CY, Bailly-Maitre B, Reed JC: Endoplasmic reticulum stress: cell life and death decisions. *J Clin Invest* 2005;115:2656-2664.
- 10 Zhao L, Ackerman SL: Endoplasmic reticulum stress in health and disease. *Curr Opin Cell Biol* 2006;18:444-452.
- 11 Sawada T, Minamino T, Fu HY, Asai M, Okuda K, Isomura T, Yamazaki S, Asano Y, Okada K, Tsukamoto O, Sanada S, Asanuma H, Asakura M, Takashima S, Kitakaze M, Komuro I: X-box binding protein 1 regulates brain natriuretic peptide through a novel AP1/CRE-like element in cardiomyocytes. *J Mol Cell Cardiol* 2010;48:1280-1289.
- 12 Tabas I: The role of endoplasmic reticulum stress in the progression of atherosclerosis. *Circ Res* 2010;107:839-850.
- 13 Minamino T, Komuro I, Kitakaze M: Endoplasmic reticulum stress as a therapeutic target in cardiovascular disease. *Circ Res* 2010;107:1071-1082.
- 14 Wu H, Ye M, Yang J, Ding J, Yang J, Dong W, Wang X: Nicorandil Protects the heart from ischemia/reperfusion injury by attenuating endoplasmic reticulum response-induced apoptosis through PI3K/Akt signaling pathway. *Cell Physiol Biochem* 2015;35:2320-2332.
- 15 Lin Y, Zhang X, Wang L, Zhao Y, Li H, Xiao W, Xu C, Liu J: Polyamine depletion attenuates isoproterenol-induced hypertrophy and endoplasmic reticulum stress in cardiomyocytes. *Cell Physiol Biochem* 2014;34:1455-1465.
- 16 de Almeida SF, Picarote G, Fleming JV, Carmo-Fonseca M, Azevedo JE, de Sousa M: Chemical chaperones reduce endoplasmic reticulum stress and prevent mutant HFE aggregate formation. *J Biol Chem* 2007;282:27905-27912.
- 17 Ozcan U, Yilmaz E, Ozcan L, Furuhashi M, Vaillancourt E, Smith RO, Görgün CZ, Hotamisligil GS: Chemical chaperones reduce ER stress and restore glucose homeostasis in a mouse model of type 2 diabetes. *Science* 2006;313:1137-1140.
- 18 Cheung WW, Ding W, Gunta SS, Gu Y, Tabakman R, Klapper LN, Gertler A, Mak RH: A pegylated leptin antagonist ameliorates CKD-associated cachexia in mice. *J Am Soc Nephrol* 2014; 25: 119-128
- 19 Ding W, Yang L, Zhang M, Gu Y: Chronic inhibition of nuclear factor kappa B attenuates aldosterone/salt-induced renal injury. *Life Sci* 2012;90:600-606.
- 20 Slatopolsky E, Weerts C, Thielan J, Horst R, Harter H, Martin KJ: Marked suppression of secondary hyperparathyroidism by intravenous administration of 1, 25-dihydroxy-cholecalciferol in uremic patients. *J Clin Invest* 1984;74:2136-2143.
- 21 Panizo S, Barrio-Vázquez S, Naves-Díaz M, Carrillo-López N, Rodríguez I, Fernández-Vázquez A, Valdivielso JM, Thadhani R, Cannata-Andía JB: Vitamin D receptor activation, left ventricular hypertrophy and myocardial fibrosis. *Nephrol Dial Transplant* 2013;28:2735-2744.
- 22 Carrillo-López N, Román-García P, Rodríguez-Rebollar A, Fernández-Martín JL, Naves-Díaz M, Cannata-Andía JB: Indirect regulation of PTH by estrogens may require FGF23. *J Am Soc Nephrol* 2009;20:2009-2017.
- 23 Zoccali C: Left ventricular systolic dysfunction: a sudden killer in end-stage renal disease patients. *Hypertension* 2010;56:187-188.
- 24 Gross ML, Ritz E: Hypertrophy and fibrosis in the cardiomyopathy of uremia-beyond coronary heart disease. *Semin Dial* 2008;21:308-318.
- 25 Gupta S, Li S, Abedin MJ, Noppakun K, Wang L, Kaur T, Najafian B, Rodrigues CM, Steer CJ: Prevention of acute kidney injury by tauroursodeoxycholic acid in rat and cell culture models. *PLoS One* 2012;7:e48950.
- 26 Lekawanvijit S, Kompa AR, Manabe M, Wang BH, Langham RG, Nishijima F, Kelly DJ, Krum H: Chronic kidney disease-induced cardiac fibrosis is ameliorated by reducing circulating levels of a non-dialysable uremic toxin, indoxyl sulfate. *PLoS One* 2012;7:e41281.

- 27 Schröder M, Kaufman RJ: The mammalian unfolded protein response. *Annu Rev Biochem* 2005;74:739-789.
- 28 Harding HP, Zhang Y, Bertolotti A, Zeng H, Ron D: Perk is essential for translational regulation and cell survival during the unfolded protein response. *Mol Cell* 2000;5:897-904.
- 29 Yamamoto K, Sato T, Matsui T, Sato M, Okada T, Yoshida H, Harada A, Mori K: Transcriptional induction of mammalian ER quality control proteins is mediated by single or combined action of ATF-6 alpha and XBP-1. *Dev Cell* 2007;13:365-376.
- 30 Harding HP, Zhang Y, Ron D: Protein translation and folding are coupled by an endoplasmic-reticulum-resident kinase. *Nature* 1999;397:271-274.
- 31 Kaufman RJ: Stress signal from the lumen of the endoplasmic reticulum: coordination of gene transcriptional and translational controls. *Genes Dev* 1999;13:1211-1233.
- 32 Mao W, Iwai C, Qin F, Liang CS: Norepinephrine induces endoplasmic reticulum stress and downregulation of norepinephrine transporter density in PC12 cells via oxidative stress. *Am J Physiol Heart Circ Physiol* 2005;288:H2381-2389.
- 33 Sadoshima J: Redox regulation of growth and death in cardiac myocytes. *Antioxid Redox Signal* 2006;8:1621-1624.
- 34 Ron D, Walter P: Signal integration in the endoplasmic reticulum unfolded protein response. *Nat Rev Mol Cell Biol* 2007;8:519-529.
- 35 Zinszner H, Kuroda M, Wang X, Batchvarova N, Lightfoot RT, Remotti H, Stevens JL, Ron D: CHOP is implicated in programmed cell death in response to impaired function of the endoplasmic reticulum. *Genes Dev* 1998;12:982-995.
- 36 Oyadomari S, Koizumi A, Takeda K, Gotoh T, Akira S, Araki E, Mori M: Targeted disruption of the Chop gene delays endoplasmic reticulum stress-mediated diabetes. *J Clin Invest* 2002;109:525-532.
- 37 Ding W, Yang L, Zhang M, Gu Y: Reactive oxygen species-mediated endoplasmic reticulum stress contributes to aldosterone-induced apoptosis in tubular epithelial cells. *Biochem Biophys Res Commun* 2012;418:451-456.
- 38 Okada K, Minamino T, Tsukamoto Y, Liao Y, Tsukamoto O, Takashima S, Hirata A, Fujita M, Nagamachi Y, Nakatani T, Yutani C, Ozawa K, Ogawa S, Tomoike H, Hori M, Kitakaze M: Prolonged endoplasmic reticulum stress in hypertrophic and failing heart after aortic constriction: possible contribution of endoplasmic reticulum stress to cardiac myocyte apoptosis. *Circulation* 2004;110:705-712.
- 39 Li Z, Zhang T, Dai H, Liu G, Wang H, Sun Y, Zhang Y, Ge Z: Endoplasmic reticulum stress is involved in myocardial apoptosis of streptozocin-induced diabetic rats. *J Endocrinol* 2008;196:565-572.
- 40 Morishima N, Nakanishi K, Takenouchi H, Shibata T, Yasuhiko Y: An endoplasmic reticulum stress-specific caspase cascade in apoptosis. Cytochrome c-independent activation of caspase-9 by caspase-12. *J Biol Chem* 2002;277:34287-34294.
- 41 Ohse T, Inagi R, Tanaka T, Ota T, Miyata T, Kojima I, Ingelfinger JR, Ogawa S, Fujita T, Nangaku M: Albumin induces endoplasmic reticulum stress and apoptosis in renal proximal tubular cells. *Kidney Int* 2006;70:1447-1455.
- 42 Nakagawa T, Yuan J: Cross-talk between two cysteine protease families. Activation of caspase-12 by calpain in apoptosis. *J Cell Biol* 2000;150:887-894.